ISSN: 0975-766X
CODEN: IJPTFI
Available Online through
www.ijptonline.com
Research Article

APPLICATION OF *PHRAGMITES* AS A BIOSORBENT FOR REMOVAL OF ACID BLUE-193 FROM WASTEWATER: KINETICS, EQUILIBRIUM, AND THERMODYNAMIC STUDIES

Tahereh Shojaeimehr[1,2], Mohammad Ali Khadivi[3], Razieh Khamutian[1], Younes Sohrabi[4], Meghdad Pirsaheb[1*]
[1]School of Public Health, Research Center for Environmental Determinants of Health (RCEDH), Kermanshah University of Medical Sciences, Kermanshah, Iran.
[2]Department of engineering, Sanandaj Branch, Islamic Ajad University, Sanandaj, Iran.
[3]Chair of Process Dynamics and Operation, Berlin Institute of Technology, Strasse des 17. Juni 135, Sekr. KWT9, D-10623 Berlin, Germany.
[4]Students research Committee, Kermanshah University of Medical Sciences, Kermanshah, Iran.
Email:mpirsaheb@yahoo.com

Received on 25-02-2016 *Accepted on 20-03-2016*

Abstract

In this paper, the feasibility of *Phragmites* as a biosorbent for removal of Acid Blue-193 (AB193) from synthetic wastewater was studied in batch experiments. The effect of various parameters such as initial concentration, temperature, initial pH, biosorbent dosage, and the contact time was investigated. The optimum conditions were found to be pH=1.5, biosorbent dosage of 50 mg, and temperature of 35℃ in the range of initial concentration from 50 to500 mg/L. The equilibrium contact time was 90 min. Also, the maximum sorption capacity of AB193 estimated from Langmuir isotherm was 111.111 (mg/g) at 35°C. The equilibrium behavior was studied by Freundlich and Langmuir isotherms. Although, both isotherms showed a good accordance, Freundlich isotherm showed the best accordance with the equilibrium data. The sorption kinetic followed from the pseudo-second-order model. The thermodynamic studies proved that the sorption process was physical, spontaneous, feasible, endothermic, and randomness process. The results demonstrate that *Phragmites* has high ability in dye removal as local and green biosorbent with easy access.

***Keywords*:** Phragmites; Acid Blue-193; Isotherm; Kinetic; Thermodynamic.

Introduction

These days the high level of production and extensive use of dyes causes to generate a large amount of colored wastewater which produces toxicological problems and environmental pollution (1, 2). Benzidine or arlyamine based dyes are well known for their carcinogenic characteristics. The treatment of these dyes due to their synthetic origins,

aromatic structure, and non-degradable nature is difficult (3). Some dyes are reported to cause allergy, dermatitis, skin irritation, cancer and mutation in human (2). Thus, the dye removal from wastewater before entrance to water sources is important object.

Removal methods of dye molecules from wastewater can be classified in many categories such as physical, chemical, biological, radiation, and electrochemical processes (4, 5). Although there are many methods for dye removal, it is difficult to treat the wastewater by using traditional methods, because most of synthetic dyes are stable to light, chemicals, biological treatment, and etc. (2). With respect to all methods, adsorption is a prevalent method for wastewater treatment due to its low-cost and easy operation, regeneration of the sorbent. Adsorption of dyes is mainly dependent on dyes properties, structure, and their surface chemistry. Activated carbon and resins are often used as common sorbent in the treatment of water contamination due to high adsorption capacity. However, the high cost of these materials limits their applications in large-scale (6-9). During the last years, extensive research has been done to find low-cost, available, and high efficiency sorbents for removal of organic and inorganic pollutants. Nowadays, investigations are proving that biosorbents, especially waste products of agricultural operations and plants are good choices as cheap and natural materials for wastewater treatment instead of commercial materials such as yellow passion fruit waste (10), Silkworm pupa (11), water-hyacinth (12), cotton(13), henna plant (14), Petuniagrandiflora and, Gailardiagrandiflora(15), powdered orange waste(16), Medicago sativa L. and SesbaniacannabinaPers(17), bamboo (18), *Fucus vesiculosus* (19), modified sphagnum peat moss (20), cashew nut shell (21), sunflower seed hull (22), and etc.

Phragmites is a large perennial grass found in wetlands throughout temperate and tropical regions such as rivers and marshes (23). Where conditions are suitable, *Phragmites* can spread at 5 meters or more per year in height. It can grow in damp ground, in standing water up to 1 meter or so deep. The height of the leaves is 20–50 centimeters and 2–3 centimeters in width.

Current work is an exhaustive study investigating the adsorption potential of Phragmites as a biosorbent for Acid Blue 193 (AB193) removal from synthetic wastewater solution under different conditions such as the initial concentration, initial pH, Sorbent dosage, temperature, and the contact time. FT-IR and FESEM measurements were employed as characterization methods. At the following step, behavior of an absorption process, including thermodynamic, kinetic, isotherm was studied. The results proved that Phragmites could be considered as green and powerful biosorbent in dye removal.

Materials and Methods

Materials

Phragmites was collected from the Sarab Niloufar lake, Kermanshah, Iran. They were gathered and cut into small pieces. It was washed with deionized water for several times to remove dust and soluble impurities. Then, it was dried under shadow to remove the moisture. After drying, it was grind by the mill. The particles with 60 mesh size (250 μm) were used as the biosorbent and were stored in desiccators. Synthetic textile dye AB193 (M_W= 416.38 (g/mol), C.I. 12392-64-2) without further purification was obtained from Booyakhsaz Co., Tabriz, Iran. Chemical structure of AB193 is depicted in Fig.1.

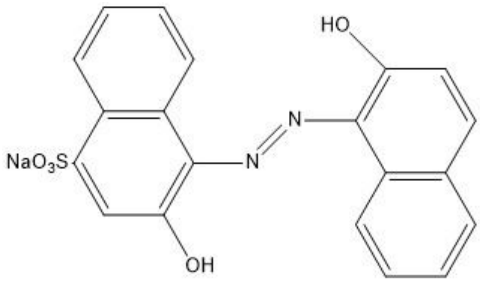

Figure-1: Chemical structure of Acid blue 193 (AB193).

Different concentrations of dye solution were prepared from a stock of 1000 mg/L solution. The various known concentrations were prepared from the stock solution. pH of the solutions was adjusted using 0.1M HNO3 and 0.1 M NaOH. All other materials were in analytical grade.

The characterization of the biosorbent

The absorbance of AB193 (at 609 nm) is measured with a Perkin–Elmer UV–Vis spectrophotometer (UNICO UV-2100). pH meter (827 pH lab Metrohm, Swiss made), shaker/incubator (DK-S1060, Korea) was used to conduct the batch experiments in desired rate, temperature, and time. Spectroscopic studies were conducted using WQS-510, China FT-IR spectrometer. The surface morphology of the biomass was shown by a field emission scanning electron microscope (FESEM, Hitachi S-4160, Japan). The elemental analysis of *Phragmites* was performed by elemental analyzer (Single-Euro EA3000).

Batch biosorption experiments

In each of batch experiments, 50 ml of the solution in the arbitrary concentration was mixed with the certain amount of the biosorbent in 250 ml Erlenmeyer flasks and then were agitated in the shaker incubator at 100 rpm and definite temperature. Then, equilibrated solution was filtered and the concentration of AB193 solutions was identified by a UV-spectrometer. Sorption capacity was determined by the following equation (24):

$$q_t = \frac{(C_0 - C_t)\cdot V}{m} \quad (1)$$

Where q_t (mg/g) are biosorption capacity at equilibrium time and at time t (3), C_0 (mg/L) and C_t (mg/L) are initial and final AB193 concentration at time t in solution, respectively. V (ml) is the solution volume, and m (mg) is the sorbent dosage.

The experiments were performed at twice and average values were reported as the results. In the next step, the equilibrium behavior of the biosorbent was studied at T=35℃, m=50 mg, pH=1.5, and the initial concentration range of 50-500 (mg/L). Adsorption kinetic was investigated for the concentration from 50 to 500 (mg/L) in the above conditions. Then, thermodynamic studies were tested in the obtained optimum conditions for temperature of 15, 25, and 35℃.

Result and Discussion

Characterization of biosorbent

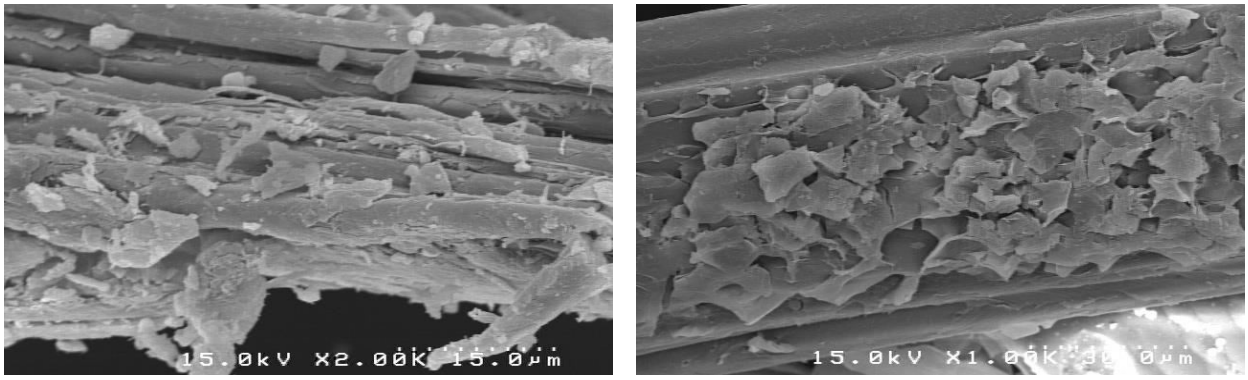

Figure-2: FESEM micrographs of *Phragmites* in two scales.

The surface morphology of *Phragmites* is shown in Fig. 2. FESEM analysis represented a fiber structure for the biomass.

FT-IR spectra of AB 193, *Phragmites*, and *Phragmites* loaded with AB193 are showed in Fig. 3.

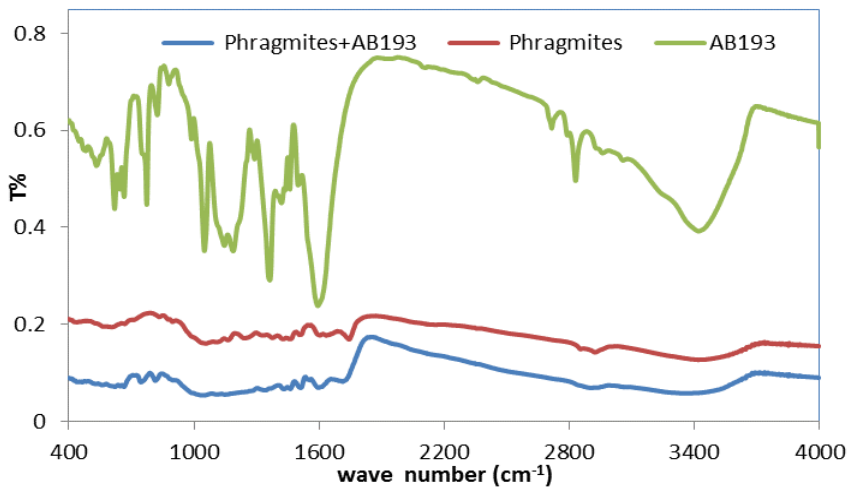

Figure-3: FT-IR spectra for *Phragmites* before and after AB193 biosorption.

Spectra of the three samples reveal the presence of several peaks of functional groups. All of them have a long stretch bandwidth around 3500–3200 cm^{-1} signifying presence of -OH and -NH functional groups, although located at different bandwidths. *Phragmites* has its –OH band width from 3300–3650 cm^{-1}. The precursor has C═O functional group peaks located on 1750 and 1615 cm^{-1}. Some C═C bands of benzene groups are located on 1500-1540 cm^{-1}.Some inorganic carbonates compounds in plane bend of C─O are found on 1458 cm^{-1}, band width 1375cm^{-1} have N─O stretch, 1055 cm^{-1} and 621 cm^{-1} band widths have some molecules containing sulfur/oxygen bonds (S═O) and silica Si─O─Si bend, respectively. *Phragmites* before adsorption have functional groups such as C─O, C═O and C═C are located between 1550 and 1650 cm^{-1} band width and some inorganic sulfates and silica Si─O─Si asymmetric stretch are found on wave number range of 600–1100 cm^{-1}. Phragmites after adsorption has some C═O and C═C groups between 1650 and 1700 cm−1 wave numbers. The presence of some amines and Nitro functional groups are located at peak numbers 1557 cm−1 (NH2), and 1540 cm−1 (NO2asymmetric stretch), 1170cm−1 (saturated secondary amine C─N stretch) which are attributed to the AB193 adsorbed on Phragmites. On the whole, band intensities were decreased after the adsorption of dye molecules on Phragmites, which support the adsorption of dye molecules on the pores Phragmite (8).

The effect of pH on biosorption capacity

pH is one of the most important parameters in dye removal(25). Changes of solution pH can change the chemical behavior of surface functional group, surface charge of sorbent, and the degree of ionization of adsorbate (3).

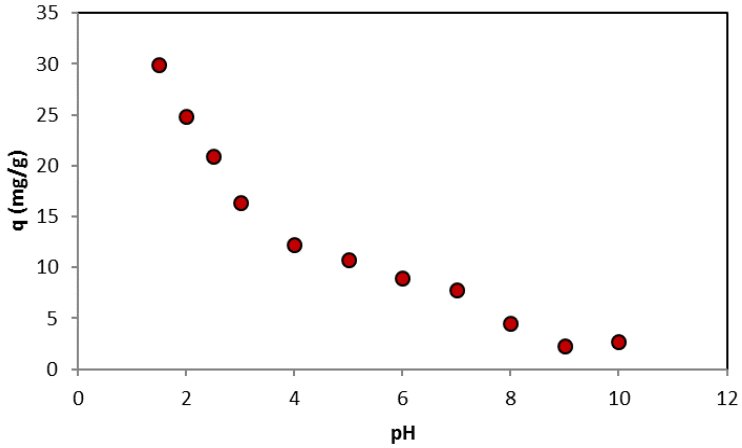

Figure-4: Effect of pH on AB193biosorption capacity onto *Phragmites* (*T*:35°C, C_0:200 (mg/L), *m/V*:1(g/L), and *t*:120 (3)).

Fig. 4 shows the effect of initial pH on AB193 sorption capacity and surface charge of biosorbent over the range from 1.5 to 10.

At low pH, the functional groups on the adsorbent surface are protonated. The decrease of pH causes a decrease in the surface charges, and likely more interactions due to electrostatic attractions between negatively charged dye anions and positively charged adsorption sites (2, 3).

The data graphed in Fig. 4 that reveals the maximum adsorption capacity AB193 (29.977 mg/g) at acidic pH of 1.5 for 200 mg/L of initial AB193 concentration at 25ºC. With the increment of pH, surface charge of sorbent increases gradually. Then, the competition between negatively charged dye anions and OH^- in the solution is leaded to decrease sorption capacity by active sites. On the other hand, the decrease of AB193 adsorption capacity may be due to repulsion between the negatively charged surface and the anionic dye molecules (2, 3).

The effect of biosorbent dosage

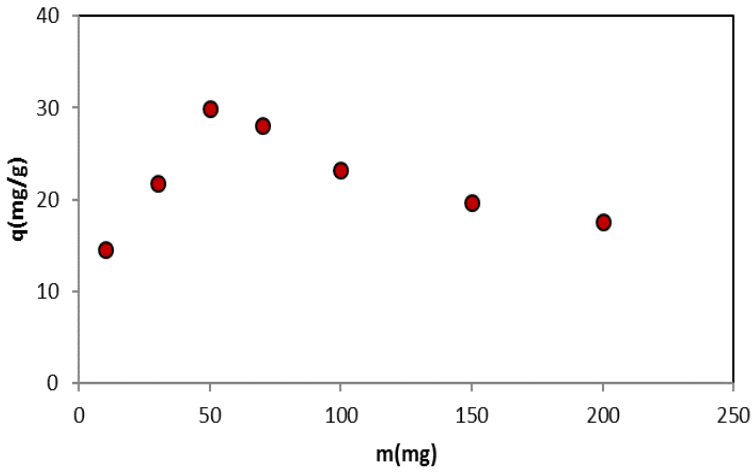

Figure-5: Effect of biosorbent dosage on AB193 biosorption capacity onto *Phragmites* (*T*:35°C, C_0:200 (mg/L), *pH*:1.5, and *t*:120 min)

The effect of biosorbent dosage is shown in Fig. 5. As can be seen in this Figure, with increasing of the biosorbent dosage from 10 to 50 mg, AB193 adsorption capacity is increased from 14.548 to 29.9771 (mg/g). After that, the increasing of biosorbent dosage from 50 mg up to 200 mg is resulted to decrease of adsorption capacity from 29.9771 to 17.634 (mg/g).

The increment of biosorbent dosage causes to increase the active adsorption sites and the number of biosorbent particles surrounding dye molecules (11, 26). But increasing more biosorbent dosage may increase the saturation sites of the sorbent during the biosorption process; also it may be concluded that in the high dosage, the biosorbent particles aggregates and diffusion path length increases (27).

Hence, the optimum amount of biosorbent dosage in the following experiments is considered as 50 mg.

The effect of the contact time and AB193 initial concentration

The sorption capacity as the function of contact time is presented in Fig. 6.

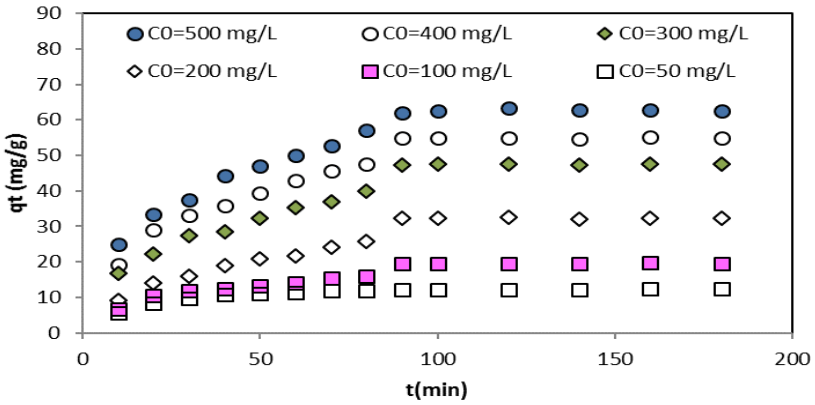

Figure-6: Effect of the contact time and initial concentration on AB193 biosorption capacity onto *Phragmites* (*T*:35°C, *pH*:1.5, *m*: 1(g/L)).

According to the figure, within the first 30 min, AB193 sorption rate is quick. It can be related to access higher active sites and high driving force (the concentration gradient) (27). After the occupation of the active adsorption sites, the sorption rate becomes slower. In this stage, AB193 molecules diffuse to the interior of the sorbent particles. According to Fig. 6, the equilibrium time is about 90 min as the optimum contact time for further experiments. After this time, the increment of the contact time did not affect sensible on adsorption capacity for all of the studied concentrations (27).

As can be seen from Fig. 6, AB193 adsorption capacity increases with the increment of the initial concentration from 50 to 500 (mg/L), significantly. This is due to the fact that at low concentrations, the ratio of surface active sites to the dye molecules in solution is high. Hence, all of dye molecules may interact with the active sites on sorbent surface. But, because of the low concentration of dye molecules in solution, sorption capacity is low (16). In high concentrations, the concentration gradient is a driving force to overcome mass transfer resistance between sorbent surface and liquid phase and also an increase in the ratio of dye molecules amount per unit weight of biosorbent (27, 28).

Biosorption thermodynamic

The change in temperature can affect on thermodynamic behavior. The thermodynamic parameters could provide inherent energetic changes during adsorption processes. The thermodynamic parameters such as enthalpy (ΔH°), entropy (ΔS°), and Gibbs free energy (ΔG°), could be calculated by the following equations (27, 29):

$$K_c = \frac{q_e}{C_e} \quad (2)$$

$$Ln(K_c) = \frac{\Delta S^\circ}{R} - \frac{\Delta H^\circ}{RT} \quad (3)$$

$$\Delta G^\circ = -RTLn(30) \quad (4)$$

Where K_c is the equilibrium constant and is calculated in different temperatures using Eq. (2). C_e and q_e are the equilibrium concentration (mg/L) and adsorption capacity (mg/g), respectively. $\Delta S°$, $\Delta H°$, and $\Delta G°$ are changes in entropy (kJ/mol. K), enthalpy (kJ/mol), and Gibbs free energy (kJ/mol), respectively. R is the gas constant (8.314 kJ/kmol.K) and T is the absolute temperature (1). The value of K_c was determined from the intercept of the plot Ln (q_e/C_e) vs. q_e in different temperatures which is depicted in Fig. 7 (29).

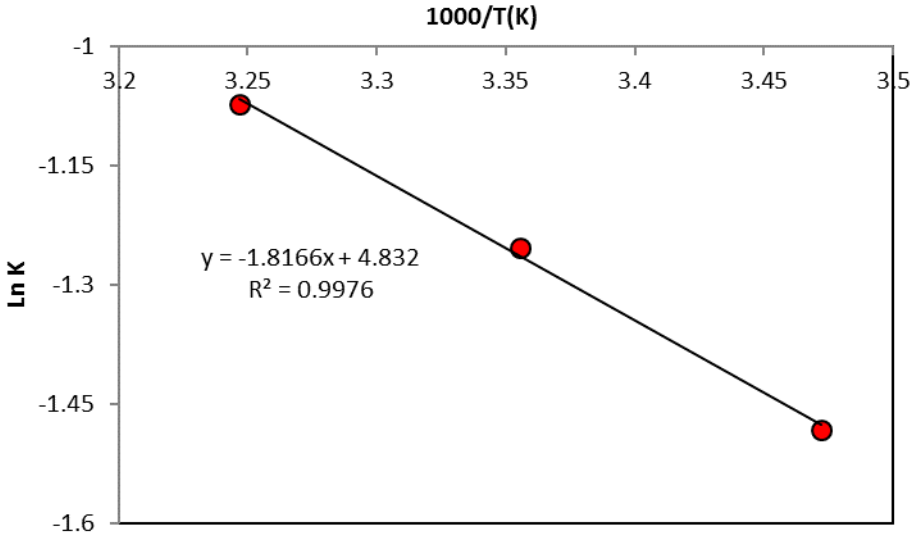

Figure-7: Effect of the temperature and initial concentration on AB193 biosorption capacity onto Phragmites (pH:5, m: 0.5 (g/L), and t: 60 min.

$\Delta S°$ and $\Delta H°$ parameters are obtained from the intercept and slope of the Van't Hoff plot of *Ln* K_c vs. *1000/T* (1) with correlation coefficient of 0.99 (31). The thermodynamic parameters are reported in Table 1.

Table-1: The value of thermodynamic parameters for biosorption of AB193 on *Phragmites.*

T(1)	K_c	$\Delta G^\circ (^{kJ}/_{mol})$	$\Delta H^\circ (^{kJ}/_{mol})$	$\Delta S^\circ (^{kJ}/_{mol.K})$
288	0.22	-3.546	15.103	0.040
298	0.286	-3.02		
308	0.342	-4.45		

According to the obtained results, the negative $\Delta H°$ value predicts an endothermic biosorption process namely, the biosorption capacity increases with the increasing of temperature from 15 to 35°C. $\Delta S°$ value is found to be positive showing the tendency of *Phragmites* to adsorb AB193 molecules and the randomness in the liquid/solid interface during the adsorption process(29, 31).

$\Delta G°$ value is negative at all of the tested temperatures that confirm a feasible and spontaneous biosorption. As be reported, $\Delta G°$ value up to -20 (kJ/mol) is in accordance with electrostatic interaction between metal ions and active sites (physical adsorption) and $\Delta G°$ values more negative of -40 (kJ⁄mol) reveal chemical adsorption (2).

According to $\Delta G°$ value obtained in this work, AB193 sorption on *Phragmites* is physical biosorption process (29, 31).

Biosorption isotherms

The relationship between equilibrium sorption capacity and equilibrium concentration in aqueous solution, in a constant temperature is explained by isotherm plots (32). Langmuir and Freundlich isotherms are studied in current work.

In Langmuir model, it is assumed that the maximum sorption capacity is happen when the monolayer of sorbent surface becomes saturation from solute molecules and these molecules don't move on sorbent surface. Also sorption energy is a constant value for all active sites (33).

The Langmuir equation is given in Eq. 5. Freundlich model is an experimental model with the assumption that various sites have different energies. This model is explained by Eq. 6:

$$q_e = \frac{q_m K_L C_e}{1+K_L C_e} \quad (5)$$

$$q_e = K_f C_e^{1/n} \quad (6)$$

Where q_m and q_e are the maximum adsorption capacity and the equilibrium amount of dye adsorbed per unit mass of sorbent (mg/g), respectively.

C_e is the equilibrium dye concentration in the solution (mg/L). K_L is Langmuir constant related to sorption capacity (L/mol).

K_f is Freundlich constant ($mol^{1-n} L^n g^{-1}$) and n is the system parameter which is explained as sorption intensity.

The experimental data are fitted with above isotherms in linear equations. The constant value of each isotherm model has been listed in Table 2.

Table-2: The isotherm model parameters evaluated for AB193biosorption.

	Langmuir Isotherm			Freundlich Isotherm		
T(1)	$q_m(^{mg}/_{g})$	$K_L(^{L}/_{mol})$	R^2	$K_f(mol^{1-n}L^n/_{g})$	n	R^2
288	105.263	0.002	0.993	0.5011	1.302	0.992
298	106.383	0.003	0.965	0.62	1.403	0.99
308	111.111	0.003	0.951	0.986	1.456	0.996

Although, two models are fitted very well with equilibrium data, Freundlich isotherm is fitted better than Langmuir isotherm.

Kinetic studies

There are three steps in the metal ion sorption process consist of mass transfer of liquid bulk (boundary layer) to the external surface of sorbent, sorption reaction on sorbent surface, and the intra-particle diffusion in pores (25). To investigate the controlling mechanism in sorption process, biosorption kinetics were studied by pseudo-first-order, pseudo-second-order and intra-particle diffusion models according to the following equations (34). The pseudo-first-order model can be expressed by (35):

$$dq_t/_{dt} = k_1(q_e - q_t) \qquad ()$$

Linear form of the pseudo-first-order model is expressed as:

$$log(q_e - q_t) = log(q_e) - \frac{k_1 t}{2.303} \qquad (8)$$

Where q_e and q_t are biosorption capacity (mg/g) at equilibrium time and at time t (3), respectively. K_1 is the rate constant of biosorption (min^{-1})

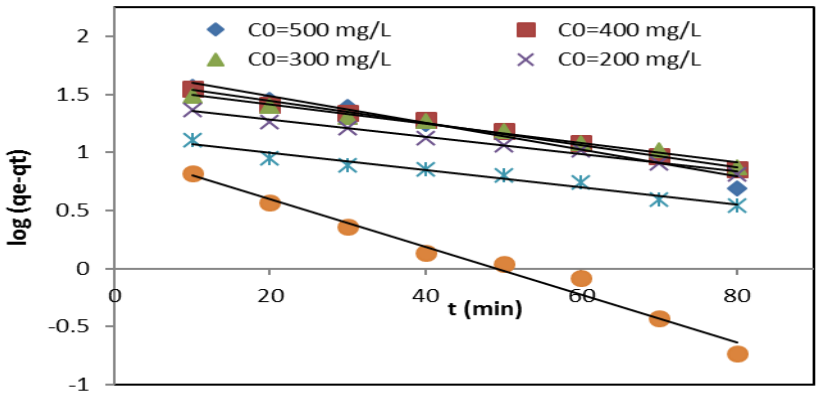

Figure-8: Pseudo-first-order kinetic model for AB193 onto Phragmites at different concentrations.

Fig. 8. shows linear plot log (q_e- q_t) versus t is obtained from Eq. (8).

The pseudo-second-order model was modeled from (24):

$$dq_t/dt = k_2(q_e - q_t)^2 \quad (9)$$

Linear form of above equation is written as:

$$t/q_t = t/q_e + 1/k_2 q_e^2 \quad (10)$$

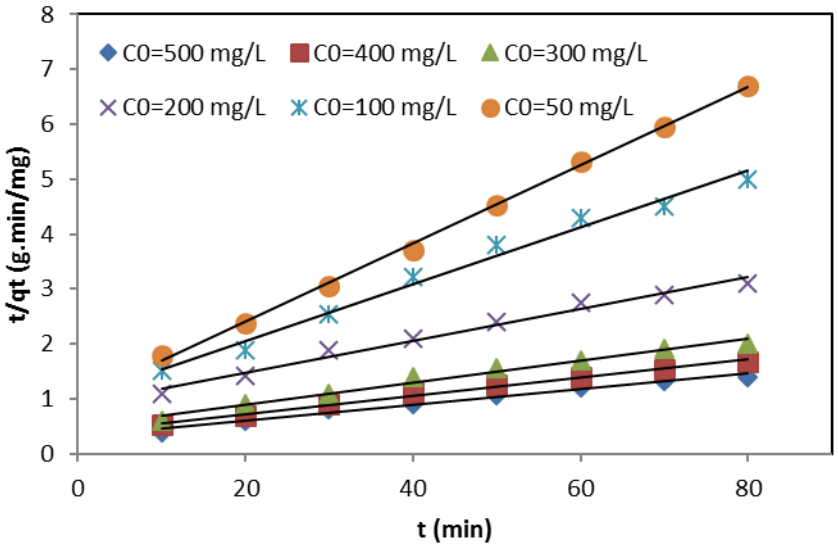

Figure-9: Pseudo-second-order kinetic model for AB193 onto Phragmites at different concentrations.

Fig. 9 shows linear plot of t/q_t vs. t. The plot slop and intercept gives q_e (mg/g) and k_2 (g/mg.min), respectively. $h=k_2q_e^2$ is the initial rate of biosorption process (mg/g.min) that is shown in Table 3.

Table-3: The kinetic parameters for AB193biosorption onto *Phragmites*.

Kinetic models		**pseudo-first-order model**			**pseudo-second-order model**				**intra-particle diffusion model**	
C_o(mg/L)	$q_{e_{exp}}$(mg/g)	k_1(min^{-1})	$q_{e_{cal}}$(mg/g)	R^2	k_2(g/mg.min)	$q_{e_{cal}}$(mg/g)	h	R^2	k_{id}(mg.$min^{0.5}$/g)	R^2
50	12.120	0.022	5.135	0.992	0.005	14.045	1.024	0.999	1.119	0.903
100	19.520	0.016	3.133	0.964	0.003	19.342	0.94	0.96	1.49	0.991
200	32.20	0.01	4.14	0.99	0.001	34.602	1.102	0.95	2.4	0.990
300	4.400	0.019	4.3	0.94	0.001	50.251	2.020	0.91	3.	0.992
400	54.00	0.022	5.135	0.992	0.001	60.241	2.540	0.991	4.19	0.96
500	62.000	0.026	5.534	0.964	0.001	69.930	3.130	0.96	5.352	0.991

To investigate the effect of diffusion resistance as a rate-controlling mechanism, intra-particle diffusion model is applied (24, 2). This model is represented by:

$$q_t = k_{id} t^{0.5} \quad (11)$$

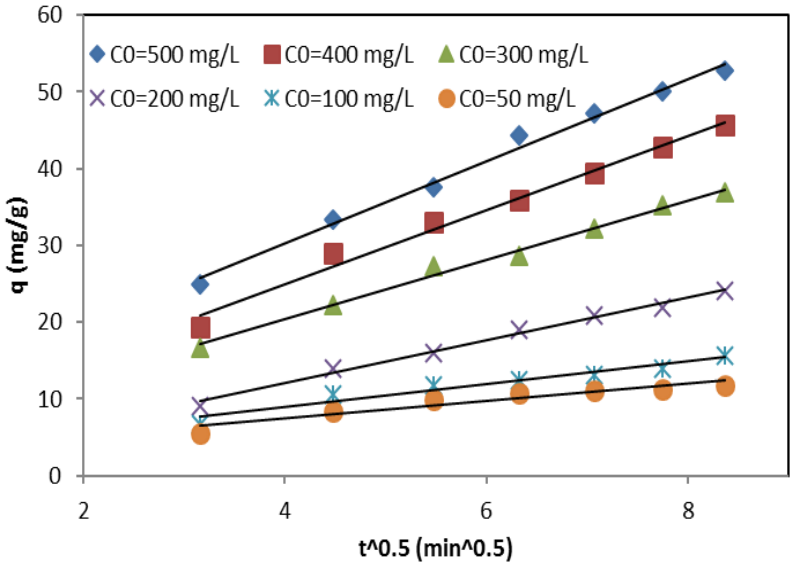

Figure-10: Intra-particle diffusion model for AB193 onto *Phragmites* at different concentrations.

Where q_t is the amount of the dye molecules adsorbed (mg/g) at time t (3), and k_{id} is the intra-particle diffusion rate constant (mg/g.min$^{0.5}$). The plot q_t vs. $t^{0.5}$ is shown in Fig. 10 and k_{id} was calculated from the slope of linear regions in the curves of Fig. 9. It can be seen; the plot q_t vs. $t^{0.5}$ was not fitted in the whole sorption regions. The initial region describes a rapid biosorption stage which is external surface sorption. The second stage is related to intra-particle diffusion region and Eq. 11 is fitted well with the data in this region. The slope of the attained line from Fig. 10 shows the intra-particle diffusion rate constant, k_{id}. The third zone belongs to the equilibrium stage when the metal ions concentration is become extremely low in the solution.

The calculated parameters and the correlation coefficients are listed in Table 3.As be seen from Table 3, the correlation coefficient of the pseudo-second-order model is higher at the studied concentrations and the obtained theoretical q_e from pseudo-second-order model agrees well with experimental q_e. The intra-particle diffusion model was fitted well with for the second region of adsorption process, only. Also it can be resulted that the intra-particle diffusion model is a rate-controlling, followed by the pseudo-second-order model. This phenomenon has been seen in previous reported researches (24, 2, 36).

The maximum sorption capacity of *Phragmites* is compared with other natural sorbents for acidic dye adsorption capacity in Table 4.

Table-4: Comparison of maximum adsorption capacity between *Phragmites* with other sorbents for removal of acid blue.

Sorbent	Dye	q_{max}(mg/g)	Reference
Aspergillusniger	Acid Blue 29	13.2	(3)
Living fungus	Acid Blue 29	6.63	(3)
Clay/Carbon mixture Acid Blue 64	Acid Blue 64	64.	(2)
Activated carbons prepared from sunflower seed hull	Acid Blue 15	110	(22)
Benzyltrimethylammonium (BTMA)-bentonite	Acid Blue 193	1043.5	(2)
Cationic polymer-loaded bentonite	Acid Scarlet GR	51.9	(3)
Cationic polymer-loaded bentonite	Acid Dark Blue 2G	40.	(3)
Anion clay Hydrotalcite	Acid Blue 29	60	(39)
Zinc aluminum hydroxide	Acid Blue 92	95	(40)
Waste tea activated carbon	Acid Blue 25	203.34	()
Na-bentonite	Acid Blue 193	6.1	(41)
Calcined alunite	Acid blue 40	60	(42)
Boron waste	Acid blue 225	15.1	(43)
Rice husk	Acid Blue	50	(44)
Phragmites	Acid Blue 193	111.111	This work

As can be seen, *Phragmites* has a good and acceptable sorption capacity relative to other biosorbents for dye removal from aqueous phase. The maximum sorption capacity of *Phragmites* was compared with other natural sorbents for AB193 removal in Table 5. As can be seen, *Phragmites* has a good and acceptable sorption capacity relative to other sorbents for AB193 removal from aqueous phase.

Conclusions

Biosorption of Acid blue 193 from synthesized wastewater by *Phragmites* in batch experiments was studied for the first time in this work. The most important conclusions from this work are summarized as follows:

- Optimum conditions were found as pH=1.5, m=50 mg, T=35°C. Under these conditions, the experimental biosorptioncapacity of AB193 was 62 (mg/g).

- Freundlich isotherm had the best correlation with experimental data.
- The maximum biosorption capacity of AB193 from Langmuir isotherm was obtained 111.111 (mg/g) at 35 °C.
- The AB193 sorption reached to equilibrium at about 90 min.
- The intra-particle diffusion model was rate-controlling for the second region of adsorption process and the kinetic biosorption was fitted well with the pseudo-second-order model.
- Biosorption of AB193 by *Phragmites* is physical, endothermic, randomness, and spontaneous process.

Acknowledgment

This letter resulted from a part of a research project No.92005 which approved by Kermanshah university of medical science.

Refrences

1. Kharat D. Preparing Agricultural Residue Based Adsorbents For Removal Of Dyes From Effluents-A Review. Brazilian Journal Of Chemical Engineering. 2015;32(1):1-12.
2. Özcan AS, Erdem B, Özcan A. Adsorption of Acid Blue 193 from aqueous solutions onto BTMA-bentonite. Colloids and Surfaces A: Physicochemical and Engineering Aspects. 2005;266(1):3-1.
3. Özcan A, Öncü EM, Özcan AS. Adsorption of Acid Blue 193 from aqueous solutions onto DEDMA-sepiolite. Journal of Hazardous Materials. 2006;129(1):244-52.
4. Ghaemi N, Madaeni SS, Daraei P, Rajabi H, Shojaeimehr T, Rahimpour F, et al. PES mixed matrix nanofiltration membrane embedded with polymer wrapped MWCNT: fabrication and performance optimization in dye removal by RSM. Journal of Hazardous Materials. 2015.
5. Souza M, Lenzi G, Colpini L, Jorge L, Santos O. Photocatalytic discoloration of reactive blue 5g dye in the presence of mixed oxides and with the addition of iron and silver. Brazilian Journal of Chemical Engineering. 2011;2(3):393-402.
6. Ould Brahim I, Belmedani M, Belgacem A, Hadoun H, Sadaoui Z. Discoloration of azo dye solutions by adsorption on activated carbon prepared from the cryogenic grinding of used tires. Chem Eng Trans. 2014;3:121-6.
7. Chen D, Zhang J, Chen J. Adsorption of methyl tert-butyl ether using granular activated carbon: Equilibrium and kinetic analysis. International Journal of Environmental Science & Technology. 2010;(2):235-42.

8. Auta M, Hameed B. Preparation of waste tea activated carbon using potassium acetate as an activating agent for adsorption of Acid Blue 25 dye. Chemical Engineering Journal. 2011;11(2):502-

9. Mahamad MN, Zaini MAA, Zakaria ZA. Preparation and characterization of activated carbon from pineapple waste biomass for dye removal. International Biodeterioration & Biodegradation. 2015.

10. Pavan FA, Lima EC, Dias SL, Mazzocato AC. Methylene blue biosorption from aqueous solutions by yellow passion fruit waste. Journal of hazardous materials. 200;150(3):03-12.

11. Noroozi B, Sorial G, Bahrami H, Arami M. Equilibrium and kinetic adsorption study of a cationic dye by a natural adsorbent—Silkworm pupa. Journal of hazardous materials. 200;139(1):16-4.

12. El-Khaiary MI. Kinetics and mechanism of adsorption of methylene blue from aqueous solution by nitric-acid treated water-hyacinth. Journal of hazardous materials. 200;14(1):2-36.

13. Bouzaida I, Rammah M. Adsorption of acid dyes on treated cotton in a continuous system. Materials Science and Engineering: C. 2002;21(1):151-5.

14. Huang J, Chu S, Chen J, Chen Y, Xie Z. Enhanced reduction of an azo dye using henna plant biomass as a solid-phase electron donor, carbon source, and redox mediator. Bioresource technology. 2014;161:465-.

15. Watharkar AD, Jadhav JP. Detoxification and decolorization of a simulated textile dye mixture by phytoremediation using Petunia grandiflora and, Gailardia grandiflora: A plant–plant consortial strategy. Ecotoxicology and environmental safety. 2014;103:1-.

16. Irem S, Khan QM, Islam E, Hashmat AJ, ul Haq MA, Afzal M, et al. Enhanced removal of reactive navy blue dye using powdered orange waste. Ecological Engineering. 2013;5:399-405.

17.Zhou X, Xiang X. Effect of different plants on azo-dye wastewater bio-decolorization. Procedia Environmental Sciences. 2013;1:540-6.

18. Guo J-Z, Li B, Liu L, Lv K. Removal of methylene blue from aqueous solutions by chemically modified bamboo. Chemosphere. 2014;111:225-31.

19.Cobas M, Sanromán M, Pazos M. Box–Behnken methodology for Cr (VI) and leather dyes removal by an eco-friendly biosorbent: F. vesiculosus. Bioresource technology. 2014;160:166-74.

20. Hemmati F, Norouzbeigi R, Sarbisheh F, Shayesteh H. Malachite green removal using modified sphagnum peat moss as a low-cost biosorbent: Kinetic, equilibrium and thermodynamic studies. Journal of the Taiwan Institute of Chemical Engineers. 2015.

21. Subramaniam R, Ponnusamy SK. Novel adsorbent from agricultural waste (cashew NUT shell) for methylene blue dye removal: Optimization by response surface methodology. Water Resources and Industry. 2015;11:64-70.

22. Thinakaran N, Baskaralingam P, Thiruvengada Ravi K, Panneerselvam P, Sivanesan S. Adsorptive removal of acid blue 15: equilibrium and kinetic study. CLEAN–Soil, Air, Water. 200;36(9):79-04.

23. Chen SH, Zhang J, Han ZJ, Zhang CL, Yue QY, editors. Adsorption of 2, 4-Dichlorophenol and Rhodamine-B from Aqueous Solutions onto Activated Carbon Derived from Phragmites Australis. Advanced Materials Research; 2015: Trans Tech Publ.

24. Visa M, Chelaru A-M. Hydrothermally modified fly ash for heavy metals and dyes removal in advanced wastewater treatment. Applied Surface Science. 2014;303:14-22.

25. Yagub MT, Sen TK, Afroze S, Ang HM. Dye and its removal from aqueous solution by adsorption: a review. Advances in colloid and interface science. 2014;209:172-4.

26. Torbati S, Khataee A, Movafeghi A. Application of watercress (Nasturtium officinale R. Br.) for biotreatment of a textile dye: Investigation of some physiological responses and effects of operational parameters. Chemical Engineering Research and Design. 2014;92(10):1934-41.

27. Shojaeimehr T, Rahimpour F, Khadivi MA, Sadeghi M. A modeling study by response surface methodology (RSM) and artificial neural network (ANN) on Cu 2+ adsorption optimization using light expended clay aggregate (LECA). Journal of Industrial and Engineering Chemistry. 2014;20(3):70-0.

28. Reddy MS, Nirmala V, Ashwini C. Bengal Gram Seed Husk as an adsorbent for the removal of dye from aqueous solutions–Batch studies. Arabian Journal of Chemistry. 2013.

29. Tahir S, Rauf N. Removal of a cationic dye from aqueous solutions by adsorption onto bentonite clay. Chemosphere. 2006;63(11):142-.

30. !!! INVALID CITATION !!!

31. Tunc Ö, Tanacı H, Aksu Z. Potential use of cotton plant wastes for the removal of Remazol Black B reactive dye. Journal of Hazardous Materials. 2009;163(1):17-9.

32. Panic VV, Velickovic SJ. Removal of model cationic dye by adsorption onto poly (methacrylic acid)/zeolite hydrogel composites: kinetics, equilibrium study and image analysis. Separation and Purification Technology. 2014;122:34-94.

33. Langmuir I. THE CONSTITUTION AND FUNDAMENTAL PROPERTIES OF SOLIDS AND LIQUIDS. PART I. SOLIDS. Journal of the American Chemical Society. 1916;38(11):2221-95.

34. Parshetti GK, Chowdhury S, Balasubramanian R. Hydrothermal conversion of urban food waste to chars for removal of textile dyes from contaminated waters. Bioresource technology. 2014;161:310-9.

35. Ho Y-S, McKay G. Pseudo-second order model for sorption processes. Process biochemistry. 1999;34(5):451-65.

36. Gao H, Zhao S, Cheng X, Wang X, Zheng L. Removal of anionic azo dyes from aqueous solution using magnetic polymer multi-wall carbon nanotube nanocomposite as adsorbent. Chemical Engineering Journal. 2013;223:84-90.

37. Fu Y, Viraraghavan T. Fungal decolorization of dye wastewaters: a review. Bioresource technology. 2001;79(3):251-62.

38. Li Q, Yue Q-Y, Su Y, Gao B-Y, Sun H-J. Equilibrium, thermodynamics and process design to minimize adsorbent amount for the adsorption of acid dyes onto cationic polymer-loaded bentonite. Chemical Engineering Journal. 2010;158(3):489-97.

39. Orthman J, Zhu H, Lu G. Use of anion clay hydrotalcite to remove coloured organics from aqueous solutions. Separation and Purification Technology. 2003;31(1):53-9.

40. Mahmoodi NM, Masrouri O, Arabi AM. Synthesis of porous adsorbent using microwave assisted combustion method and dye removal. Journal of Alloys and Compounds. 2014;602:210-20.

41. Özcan AS, Erdem B, Özcan A. Adsorption of Acid Blue 193 from aqueous solutions onto Na–bentonite and DTMA–bentonite. Journal of Colloid and Interface Science. 2004;280(1):44-54.

42. Özacar M, Şengil İA. Adsorption of acid dyes from aqueous solutions by calcined alunite and granular activated carbon. Adsorption. 2002;8(4):301-8.

43. Atar N, Olgun A. Removal of basic and acid dyes from aqueous solutions by a waste containing boron impurity. Desalination. 2009;249(1):109-15.

44. Mohamed MM. Acid dye removal: comparison of surfactant-modified mesoporous FSM-16 with activated carbon derived from rice husk. Journal of Colloid and Interface Science. 2004;272(1):28-34.

Corresponiding Author:

Meghdad Pirsaheb*,

Email:*mpirsaheb@yahoo.com*